A two-step approach for differentiating δ-ferrite and martensite in steels using EBSD

S.I. Borisov, P.D. Dolzhenko, I.S. Nikitin, A.A. Kalinenko, I.S. Zuiko, S.Yu. Mironov* *Email: S-72mail.ru

Belgorod National Research University, Belgorod 308015, Russia

1. Introduction

Due to the specific nature of the additive laser powder bed fusion (LPBF) technology, the manufactured material experiences a non-trivial thermal history involving an extremely high cooling rate (~10^6 K/s) and a pronounced thermal cycling, including several melting-to-solidification sequences. In the martensitic steels, LPBF often gives rise to the complex microstructures consisting of an intermixture of d-ferrite, austenite, and martensite [3-20]. To ascertain the key microstructural mechanisms involved in the LPBF process as well as to predict the service properties of LPBFed parts, a quantification of these phases is necessary. However, while a detection of the austenitic phase is rather straightforward, the differentiation between the d-ferrite and martensite is challenging because of the similarity of the crystal structure of the phases.

To surmount this issue, several approaches based on the electron backscatter diffraction (EBSD) technique have been proposed in the scientific literature [15, 16, 21-30]. Typically, those are based on the presumed distinction of the stored energy between the ferrite and martensite and the concomitant difference in the lattice imperfections. Hence, the distribution of a related EBSD metric (which is sometimes referred to as the image quality index, IQ) should be either bimodal or exhibit a clear transition from one phase to another. From the authors' experience, however, the experimental distributions of image quality (IQ) index are often smooth and show no clear transition between the phases. Therefore, the resulting microstructure partitioning is not always perfect.

To enhance the efficiency of this procedure, a *two-step approach* was suggested in the present study. In this case, the conventional IQ-based partitioning technique is complemented by an additional filtration step, which is based on another distinct characteristic of the martensitic phase. The latter one may include a relatively low confidence index of diffraction patterns, a broader grain orientation spread, or a finer grain size. It was assumed that such a two-factor data filtration strategy would increase the efficiency of phase partitioning. This work was undertaken to investigate the validity of this concept.

2. Experimental

The program material used in this work was a commercial 17-4 PH martensitic steel. The material was produced by 3D Systems Inc. using the nitrogen-gas atomization technique and supplied as an atomized metallic powder. The powder particles had a nearly spherical morphology and often contained satellites. The particle size distribution was relatively broad, spanning from ~1 μm to ≈30 μm.

The LPBF process was carried out on a ProX DMD 200 machine (3D Systems). To minimize porosity, LPBF variables were selected to provide a relatively high volumetric energy density. Those included a laser power of 180 W, a laser scanning speed of 1 m/s, a hatch distance of 50 μm, and a powder layer thickness of 30 mm (the volumetric energy density of 120 J/mm^3). A cuboidal-shaped sample with dimensions 10×10×20 mm^3 was built vertically using a nitrogen atmosphere. A simple parallel scan strategy was employed with a 90° rotation of the laser scan direction from layer to layer.

For EBSD observations, the built sample was sectioned in half along the building direction, mounted, and mechanically polished using standard metallographic procedures. A final surface finish was achieved using 24-h vibratory polishing with OP-S colloidal silica suspension. EBSD analysis was performed employing an FEI Quanta 600 field-emission-gun scanning electron microscope (FEG-SEM) equipped with TSL OIM™ software. Given the above-mentioned difficulty of discriminating ferrite from martensite in EBSD, these two phases were indexed as the generic body-centered cubic (BCC) phase; accordingly, the austenite was indexed as the generic face-centered cubic (FCC) phase.

3. Results and Discussion

3.1. Preliminary analysis

The EBSD IQ map of a typical microstructure evolved in the central part of the built sample is shown in Fig. 1a. In the map, the FCC phase is highlighted with red, while the BCC component is shown in gray.

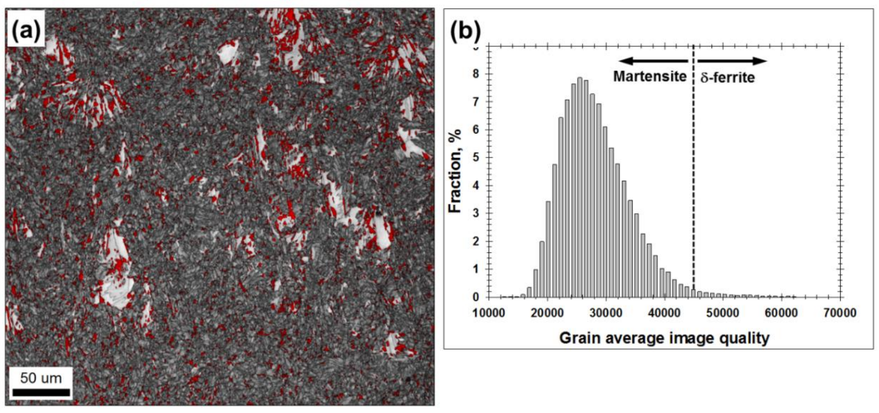

Figure 1. (a) EBSD image-quality map of evolved microstructure (austenitic phase is highlighted with red) and (b) the distribution of the grain average image-quality index derived from the BCC microstructural component and used for the separation of martensite and δ-ferrite. In (b), a presumed transition from martensite to δ-ferrite is shown.

In the context of the present study, of particular interest was the BCC microstructure. To a first approximation, it consisted of two distinct components, viz., coarse-grained and fine-grained ones.

The coarse-grained BCC component often exhibited columnar grain morphology and a comparatively bright IQ contrast (i.e., the low stored energy). Hence, this microstructural constituent was likely δ-ferrite. Contrarily, the fine-grained BCC component showed a lath-shaped morphology and a comparatively dark IQ contrast (i.e., the high stored energy). From a broad perspective, therefore, this microstructural constituent reflected martensite.

3.2. Microstructure partitioning. Step 1

To discriminate the δ-ferrite and martensite phases, the conventional IQ-based technique was first applied. The distribution of the grain average IQ indexes derived from the BCC microstructural constituent is presented in Fig. 1b. The distribution was not bimodal but exhibited a distinct asymmetry. Specifically, it consisted of a pronounced peak at a comparatively low IQ index and an extreme end in the high IQ range. It was highly likely that the former characteristic represented martensite, while the latter one reflected δ-ferrite. However, the transition between the phases was smooth, and no clear threshold could be found.

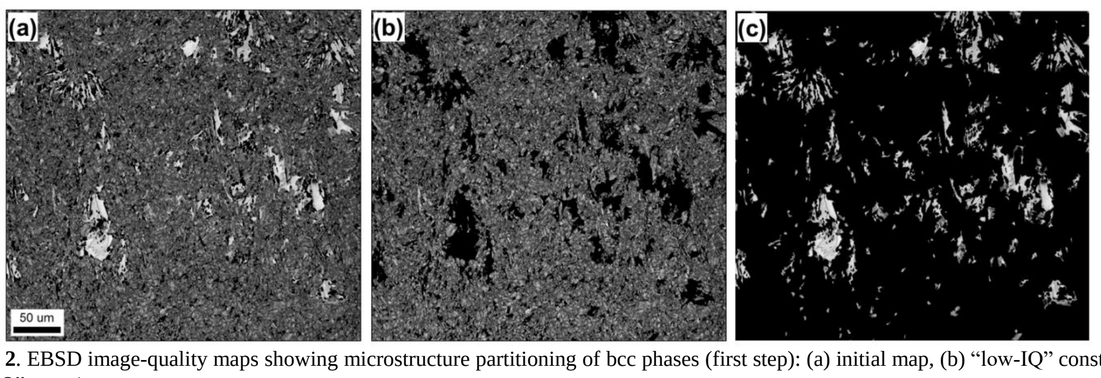

Figure 2. EBSD image-quality maps showing microstructure partitioning of bcc phases (first step): (a) initial map, (b) "low-IQ" constituent, and (c) "high-IQ" constituent.

Using a trial-and-error approach, the approximate threshold was defined at IQ = 45,000. For clarity, this presumed borderline between the phases was indicated by a dotted line in Fig. 1b. Based on this threshold, the IQ map for the BCC crystals (Fig. 2a) was partitioned into two microstructural components, as shown in Figs. 2b and c. It was found that the grains with relatively low IQ index (IQ < 45,000) exhibited lamellar morphology and comparatively fine sizes (Fig. 2b). On the other hand, the data with a higher IQ index (IQ ≥ 45,000) encompassed all coarse columnar-shaped grains but also included a fraction of fine-scale grains (Fig. 2c).

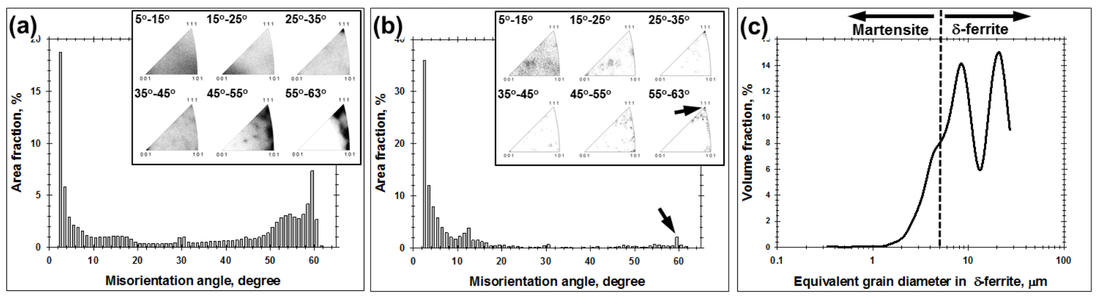

Figure 3. Misorientation distributions derived from the partitioned phases (first step): (a) "low-IQ" microstructural constituent, (b) "high-IQ" microstructural constituent, and (c) grain-size distribution of the "high-IQ" microstructural constituent. In (a) and (b), misorientation-axis distributions are shown as inserts in the top right corners. In (b), arrows show an increased fraction of nearly-60°<111> boundaries, which presumably belonged to martensitic phase. In (c), a presumed transition from martensite to δ-ferrite is shown.

To get additional insight into the partitioning results, misorientation distributions for both microstructural constituents were measured, as shown in Figs. 3a and b.

The "low IQ" constituent showed a bimodal misorientation-angle distribution with a pronounced low-angle maximum and a broad peak in the range of 50-60° (Fig. 3a). Importantly, the misorientation axes of low-angle boundaries (LABs) tended to cluster near <101>, while those of the 50-60° boundaries preferentially concentrated near <111> and <101> (insert in the top right corner of Fig. 3a). The broadly similar misorientation distributions are normally observed in martensitic structures and are usually attributable to the dominance of the boundaries between martensite variants. Therefore, almost certainly, the "low IQ" microstructural constituent represented martensite.

The misorientation-angle distribution of the "high-IQ" microstructural constituent was dominated by low-angle boundaries but also included a subtle fraction of nearly 60°<111> boundaries (Fig. 3b). While the increased LAB content could readily be associated with the dendritic origin of δ-ferrite, the 60°<111> misorientations are hard to attribute to this phase. Hence, those likely belonged to martensite, and therefore the partitioned δ-ferrite was probably contaminated by some fraction of this phase.

3.3. Microstructure partitioning. Step 2

Therefore, in accordance with expectations, the IQ-based approach was not entirely efficient. One probable reason for this effect could be the high residual stresses, which were presumably produced within the d-ferrite phase due to an extremely high cooling rate during the LPBF process. This should degrade Kikuchi patterns and thus reduce the IQ index.

Accordingly, the second partitioning step was applied. To this end, the grain size approach was used hereafter as the second data filtration step. This method was grounded on the presumed distinction in grain size between the δ-ferrite dendrites and martensite laths.

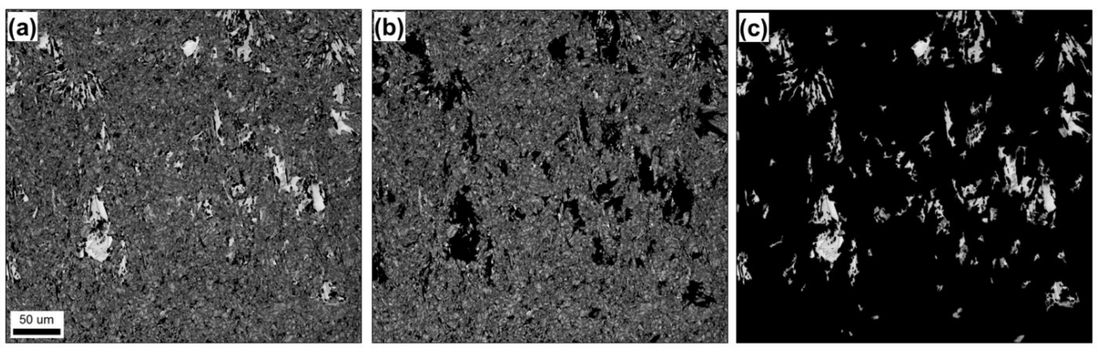

Figure 4. EBSD image-quality maps showing microstructure partitioning of bcc phases (second step): (a) initial map, (b) partitioned martensite, and (c) partitioned δ-ferrite.

The grain size distribution derived from the partitioned δ-ferrite structure was shown in Fig. 3c. Considering the specific character of the distribution, the grains below 5 μm in size were assumed to belong to the martensitic phase. For clarity, this presumed borderline between the martensite and δ-ferrite was indicated by a dotted line in Fig. 3c. Based on this threshold, the IQ map for the BCC crystals (Fig. 4a) was partitioned into two microstructural components, as shown in Figs. 4b and 4c. The misorientation distributions for the partitioned components were given in Fig. 5.

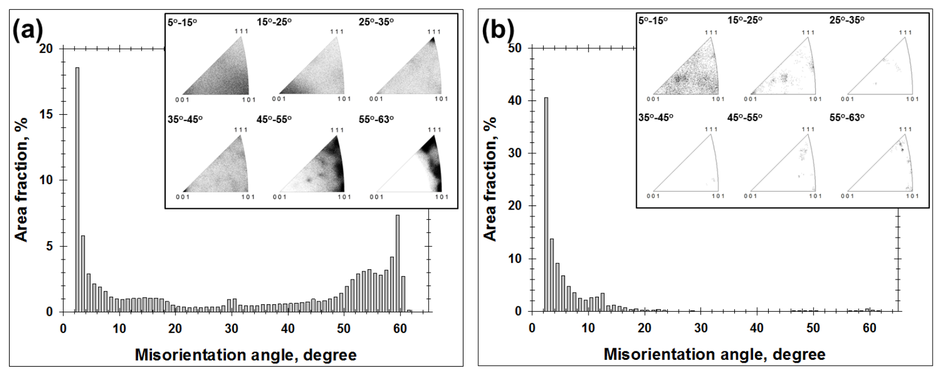

Figure 5. Misorientation distributions derived from the partitioned phases (second step): (a) martensite and (b) δ-ferrite. In both cases, misorientation-axis distributions are shown as inserts in the top right corner.

The second filtration step provided no apparent changes in either morphology or misorientation distribution of the presumed martensitic phase (Figs. 4b and 5a). In δ-ferrite, in contrast, the finest grains were filtered out (compare Figs. 4c and 2c). This eliminated the 60°<111> peak in the misorientation distribution (compare Figs. 5b and 3b). Premised on the latter observation, it was suggested that the δ-ferrite was filtered out from the martensite contaminations.

4. Summary

A two-step approach was proposed for the partitioning of the δ-ferrite and martensite phases. This method was based on EBSD and involved a two-factor data filtration according to the distinct differences between the δ-ferrite and martensite in stored energy and grain size. The stored energy within the phases was evaluated employing a so-called image quality index, i.e., the EBSD metric characterizing the sharpness of the Kikuchi bands in digitized diffraction patterns. It was found the microstructure partitioning based on the stored energy only was not entirely effective. This observation was attributed to the high residual stresses, which were presumably produced within the δ-ferrite phase due to an extremely high cooling rate during the LPBF process. In contrast, the second-step partitioning on the basis of the grain size difference between the δ-ferrite and martensite was found to be effective for distinguishing these phases.

Acknowledgements

The work was supported by the government assignment FZWG-2026-0005 "Development of scientific foundations for optimization of selective laser melting and subsequent heat treatment of precipitation-hardening martensitic steel 17-4 PH", Ministry of Science and Higher Education of the Russian Federation.